Biometals (2019) 32:939–948
https://doi.org/10.1007/s10534-019-00224-1

Structural and solution chemistry, antiproliferative effects, and serum albumin binding of three pseudohalide derivatives of auranofin

Damiano Cirri · Maria Giulia Fabbrini · Lara Massai · Serena Pillozzi · Annalisa Guerri · Alessio Menconi · Luigi Messori · Tiziano Marzo · Alessandro Pratesi

Received: 6 September 2019 / Accepted: 30 October 2019 / Published online: 19 November 2019

Abstract Three pseudohalide analogues of the established gold drug auranofin (AF hereafter), of general formula Au(PEt$_3$)X, i.e. Au(PEt$_3$)CN, Au(PEt$_3$)SCN and Au(PEt$_3$)N$_3$ (respectively denoted as AFCN, AFSCN and AFN$_3$), were prepared and characterized. The crystal structure was solved for Au(PEt$_3$)SCN highlighting the classical linear geometry of the 2-coordinate gold(I) center. The solution behaviour of the compounds was then comparatively analysed through ^{31}PNMR providing evidence for an acceptable stability under physiological-like conditions. Afterward, the reaction of these gold compounds with bovine serum albumin (BSA) and consequent adduct formation was investigated by ^{31}PNMR. For all the studied gold compounds, the [Au(PEt$_3$)]$^+$ moiety was identified as the reactive species in metal/protein adducts formation. The cytotoxic effects of the complexes were subsequently measured in comparison to AF against a representative colorectal cancer cell line and found to be still relevant and roughly similar in the three cases though far weaker than those of AF. These results show that the nature of the anionic ligand can modulate importantly the pharmacological action of the gold-triethylphosphine moiety, affecting the cytotoxic potency. These aspects may be further explored to improve the pharmacological profiles of this family of metal complexes.

Electronic supplementary material The online version of this article (https://doi.org/10.1007/s10534-019-00224-1) contains supplementary material, which is available to authorized users.

Tiziano Marzo and Alessandro Pratesi are equally contributed to this work.

D. Cirri (✉) · M. G. Fabbrini · L. Massai · A. Guerri · L. Messori (✉)
Department of Chemistry, University of Florence, Via della Lastruccia 3, 50019 Sesto Fiorentino, Italy
e-mail: damiano.cirri@unifi.it

L. Messori
e-mail: luigi.messori@unifi.it

S. Pillozzi · A. Menconi
Department of Experimental and Clinical Medicine, University of Florence, Viale GB Morgagni 50, 50134 Florence, Italy

T. Marzo
Department of Pharmacy, University of Pisa, Via Bonanno Pisano 6, 56126 Pisa, Italy

A. Pratesi
Department of Chemistry and Industrial Chemistry, University of Pisa, Via G. Moruzzi 13, 56124 Pisa, Italy

Keywords Metal based drugs · NMR · Cancer · Protein metalation · BSA

Introduction

The huge costs of new drug development represent a discouraging factor for the obtainment of new anticancer molecules. For this reason, in recent years, chemists working in the field of drug discovery have focused their interest towards drug repurposing strategies (Pushpakom et al. 2019). Indeed, the drug repositioning approach i.e. the use of an already approved drug for different indications, can be a straightforward and convenient way for discovering new active molecules. This is made possible because the investigated molecules have already passed clinical trials and may thus be considered as "safe" in this context. In this frame, a very promising metal-based compound that has attracted increasing attention as a potential anticancer chemotherapy agent is AF (Ridaura®), an orally administered gold-based drug in clinical use for the treatment of a few severe forms of rheumatoid arthritis since 1988 (Roder and Thomson 2015; May et al. 2018). In recent years, several papers have been published highlighting the antineoplastic activity of AF against several cancer models with an acceptable systemic toxicity (Landini et al. 2017; Hou et al. 2018). Based on its promising features, AF has entered clinical trials in the U.S. against various liquid and solid tumours (Marzo et al. 2019; Database of privately and publicly funded clinical studies conducted around the world.).

One of the most important mechanisms for AF anticancer activity relies in the impairment of key enzymes responsible for the maintenance of the redox homeostasis of cells. Among them, thioredoxin reductase bears a selenocysteine moiety in the active redox site that is reputed as the main site for gold coordination eventually causing potent protein inhibition (Fabbrini et al. 2019). However, it is nowadays widely ascertained that also other proteins may react with AF modulating its bioavailability and biodistribution. Serum albumin is the most abundant plasma protein and it is able to react with AF even upon short incubation times (Blocka et al. 1986; Massai et al. 2019). As a consequence, human serum albumin (HSA) turns out to be the major carrier for AF in the blood (Talib et al. 2006). Indeed, this protein is the most abundant protein in plasma, with a concentration of approximately 0.6 mM (Fanali et al. 2012). Its main physiological functions include maintenance of the pH and osmotic pressure of plasma, and transport of a variety of endogenous and exogenous substances, including metal ions (Marcon et al. 2003; Singh et al. 2018). Serum albumin consists of a single polypeptide chain of 585 amino acids including 35 cysteine residues, all of which except Cys34 are normally involved in disulfide bonds. Indeed, the unique cysteine residue Cys34 is present either as a free thiol ($\sim$ 40%), or bound to an endogenous thiol such as cysteine, homocysteine or glutathione (Lee and Wu 2015). The peculiar topology of the Cys34 site accounts for its unambiguous involvement in Au(I) (i.e. AF) and Pt(II) (i.e. cisplatin) complexes formation (Sokolowska et al. 2009).

A convenient way to extend the drug repurposing approaches for new drug discovery is to slightly modify the structure of already known active molecules, leaving unaltered the interaction abilities with serum proteins that are typical of the Au(I) complexes (Pratesi et al. 2018). Starting from these premises our research group had previously screened two derivatives of AF in which the thiosugar moiety had been replaced with chloride and iodide respectively obtaining some interesting results (Marzo et al. 2017, 2019). In this frame, we have decided to further expand the panel of AF derivatives. We also realised that satisfactory biological reports focused on the binding to serum albumin of AF pseudohalide analogues were missing in the literature. For these reasons, we decided to synthesize and fully characterise three compounds (Fig. 1), with a common chemical structure based on $Au(PEt_3)X$, where X is a pseudohalide group (–CN; –SCN or $–N_3$). The study is aimed to elucidate the stability of these gold compounds in physiological like buffers, to assess their solution behaviour in comparison with AF when incubated with a thiol-bearing protein such bovine serum albumin (BSA) and to determine their antiproliferative actions in vitro.

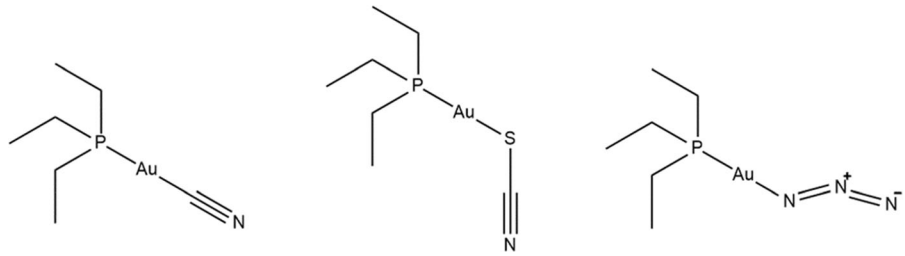

Fig. 1 Chemical structure of the investigated compounds

Materials and methods

General

All materials were purchased from Sigma-Aldrich, Merck or Honeywell and were used without further purification. LogP was determined through shake-flask method. The quantitation of compounds in the pre-saturated water or octanol phase was carried out by ICP-AES analysis following a procedure already established in our lab (Cirri et al. 2017).

Synthesis and characterization

AFCN was synthesized according to the procedure reported in Scheme 1a, using a ligand scrambling reaction. The desired product was obtained by an extraction process from water/low polarity solvent (such as chloroform) mixture. AFSCN and AFN_3 were prepared as displayed in Scheme 1b, through activation of the gold-triethylphosphine moiety with silver nitrate. All the synthesized products were characterized by elemental analysis and ^{31}PNMR.

AFCN

AFCN was synthesized using the scrambling reaction reported in literature (Hormann-Arendt and Shaw 1990). In a flask were added 5 mL of chloroform, 2 mL of MilliQ water, 31.08 mg (0.066 mmol; 1 eq.) of $[Au(PEt_3)_2]Cl$ and 21.00 mg (0.073 mmol; 1.11 eq.) of $K[Au(CN)_2]$ (both compounds were previously synthesized as described in Marzo et al. (2018). The biphasic mixture was stirred at room temperature for 4 h, then the organic phase was recovered using a separation funnel and dried under vacuum. The crude product was dissolved in 0.5 mL of $CHCl_3$ and precipitated as white small crystals immediately after adding 5 mL of Et_2O (26.8 mg; 59.3% yield). Characterization was carried out by ^{1}H, ^{13}C and ^{31}PNMR. The purity of product was assessed by CHN analysis: [calculated C: 24.65%, H: 4.43%, N: 4.11%; experimental C: 24.72%, H: 4.54%, N: 3.89%].

LogP: 0.8

^{1}HNMR ($CDCl_3$; 400.13 MHz): 1.84 (dq; J_{HH} = 7.68 Hz; J_{PH} = 9.86 Hz; 6H); 1.21 (dt; J_{HH} = 7.65 Hz; J_{PH} = 18.59 Hz; 9H)

^{31}PNMR ($CDCl_3$; 161.98 MHz): 36.05

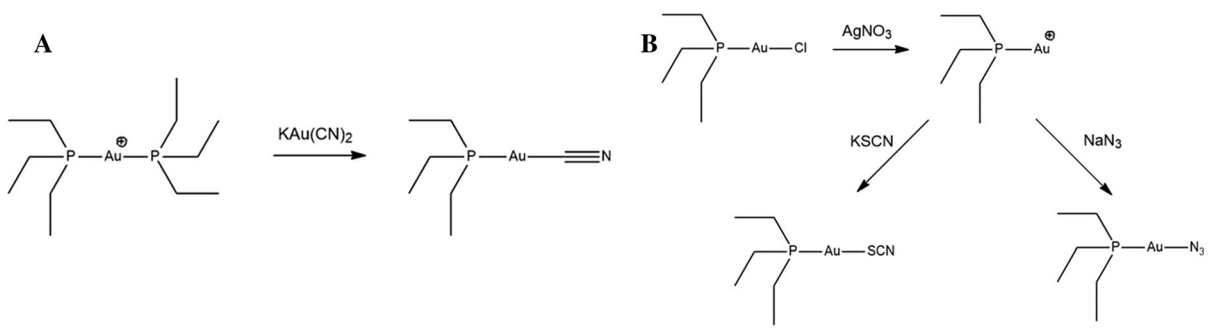

Scheme 1 Reaction pathways for the synthesis of AFCN, AFSCN and AFN_3

^{13}CNMR ($CDCl_3$; 100.61 MHz): 159.39; 18.16 (d; J_{CP} = 34.58 Hz); 9.52

AFSCN

AFSCN was synthesized modifying an existing experimental protocol (El-Etri and Scovell 1990). In a flask were added 39.45 mg of Au(PEt_3)Cl (0.112 mmol; 1 eq.), 5 mL of EtOH and 19.12 mg of $AgNO_3$ (0.112 mmol: 1 eq.). The suspension was stirred for 1 h at 25 °C and filtered to remove the AgCl formed. The liquid phase was moved in a clean flask and 10.49 mg (0.108 mmol; 0.96 eq.) of KSCN were added. The suspension was stirred for 1.5 h and dried under vacuum. The crude product was dissolved in 5 mL of dichloromethane and 5 mL of H_2O. The biphasic mixture was moved in a separation funnel and the organic phase was recovered. The aqueous phase was re-extracted with 5 mL of dichloromethane and the recovered organic ones were diluted with 7 mL of chloroform and washed with 5 mL of MilliQ water. The organic phase was then dried with $MgSO_4$ and evaporated under vacuum. The crude product was solubilized in 0.5 mL of dichloromethane and 5 mL of diethyl ether were added and the flask was kept at − 20 °C for 72 h. After this time some white crystals were formed at the bottom of the flask. Next, 10 mL of hexane were added and the flask was kept at − 20 °C for further 24 h. 25.25 mg of white crystals of the desired product were collected (yield 60.1%). Characterization was performed by ^{1}H, ^{13}C, ^{31}PNMR and X-Ray crystallography. The purity of product was assessed by CHN analysis: [calculated C: 22.53%, H: 4.05%, N: 3.75%; experimental C: 22.52%, H: 4.25%, N: 3.50%].

LogP: 0.6

^{1}HNMR ($CDCl_3$; 400.13 MHz): 1.89 (dq; J_{HH} = 7.66 Hz; J_{PH} = 10.06 Hz; 6H); 1.23 (dt; J_{HH} = 7.64 Hz; J_{PH} = 19.00 Hz; 9H)

^{31}PNMR ($CDCl_3$; 161.98 MHz): 36.63

^{13}CNMR ($CDCl_3$; 100.61 MHz): 18.48 (d; J_{CP} = 35.04 Hz); 9.66

AFN_3

AFN_3 was synthesized modifying the procedure described in literature (El-Etri and Scovell 1990). In a flask were added 53.91 mg (0.154 mmol; 1 eq.) of Au(PEt_3)Cl, 4 mL of EtOH and 26.12 mg of $AgNO_3$ (0.154 mmol; 1 eq.). The suspension was stirred for 1 h at r.t. and AgCl filter-off. The liquid phase was moved in a flask and 10.01 mg (0.154 mmol; 1 eq.) of NaN_3 were added. The suspension was stirred for 2 h at r.t., then 10 mL of hexane were added. After 10 min of stirring the suspension was filtered once again for the removal of formed $NaNO_3$, then further 10 mL of hexane were added. The flask was kept at − 20 °C for 24 h, after this time, crystals were formed at the bottom of flask. The product was recovered as 30.18 mg of white crystals (yield 54.9%). Characterization was performed by ^{1}H, ^{13}C and ^{31}PNMR. The purity of product was assessed by CHN analysis: [calculated C: 20.18%, H: 4.23%, N: 11.77%; experimental C: 19.80%, H: 3.86%, N: 10.68%].

LogP: 0.6

^{1}HNMR ($CDCl_3$; 400.13 MHz): 1.82 (dq; J_{HH} = 7.66 Hz; J_{PH} = 10.20 Hz; 6H); 1.19 (dt; J_{HH} = 7.63 Hz; J_{PH} = 18.75 Hz; 9H)

^{31}PNMR ($CDCl_3$; 161.98 MHz): 28.78

^{13}CNMR ($CDCl_3$; 100.61 MHz): 19.30 (d; J_{CP} = 37.25 Hz); 10

NMR studies

All NMR spectra were recorded on a Bruker Avance III spectrometer equipped with a Bruker Ultrashield 400 Plus superconducting magnet. Measurements took place at 400.13 MHz (^{1}H) 161.98 MHz (^{31}P) and 100.61 MHz (^{13}C).

X-ray analysis

X-ray diffraction data were collected on an Oxford Diffraction Xcalibur3 instrument with Mo Kα radiation (λ = 0.71073 Å) and at a temperature of 100 K. The software suite CrysAlisPro (CrysAlisPro 1.171.38.41r 2015) was then used for the data collection and data reduction. Absorption correction was applied with the program SCALE3 ABSPACK, also integrated in the CrysAlisPro package.

The structure was solved by using the direct methods implemented in Sir97 program (Altomare et al. 1999) and refined by full-matrix least-squares techniques using SHELXL-2013 (Thorn et al. 2012) with anisotropic displacement parameters for all non-hydrogen atoms. The hydrogen atoms in AFSCN were introduced in calculated positions and refined considering a riding model with isotropic thermal

parameters. After the final refinement, due to the presence of heavy atoms in the molecule and to a not high redundancy, some residual electron density can still be found in the map. Geometrical calculations were performed by using the program PARST (Nardelli 1995) and molecular plots were produced with ORTEP3 (Farrugia 1997), both implemented in the Crystal Structure crystallographic software package WINGX (Farrugia 2012).

All the crystal data and refinement parameters shown in Tables S1 and S2. CCDC 1910813 contains the supplementary crystallographic data for this paper. These data can be obtained free of charge from the Cambridge Crystallographic Data Centre via http://www.ccdc.cam.ac.uk/Community/Requestastructure.

Cell cultures

HCT116 cells were cultured in RPMI-1640 medium with 10% Fetal Bovine Serum (FBS), at 37 °C in humidified atmosphere and 5% CO_2 in air. Drugs were solubilised in DMSO prior to be used for biological experiments at 30 mM concentration. The subsequent solutions resulted by dilutions in accurate volumes of RPMI medium.

Cell viability assay

Cell lines were plated in 96-well plates at a cell density of 1×10^4 per well in RPMI complete medium. Cells were incubated for 24 h at 37 °C, before the compounds were added at 0, 180 nM, 250 nM, 500 nM, 1 μM. Then, cells were further incubated for 24 h at 37 °C. Finally, cells were harvested, and alive cells were counted using a haemocytometer through the Trypan Blue exclusion assay. The tests were set in triplicate and values were obtained averaging them.

Results and discussion

Synthesis and characterisation

The three compounds were synthesised according to the procedure described in the experimental section and obtained in high purity and high yield. The quality of the obtained products was characterised through a variety of analytical determinations and physicochemical measurements as reported in the experimental section.

Crystal structure of AFSCN

In the case of AFSCN, crystals suitable for X-ray diffraction analysis were obtained and the corresponding crystal structure solved. The asymmetric unit (a.u.) contains two molecules of the gold complex. The metal ion in both molecules is linearly coordinated being the angles 177.61(11)° and 172.78(14)° respectively for P(1)–Au(1)–S(1) and P(2)–Au(2)–S(2). Bond length and angles are in the range of similar compounds retrieved in the CSD (v. 5.39 November 2017 + 3 updates) (Allen 2002).

The intermetallic distance Au(1)–Au(2) between the two molecules is 3.4579(7) Å, which is frequently found in this kind of linear complexes (CSD) (Fig. 2).

Solution behaviour

The solution stability of the three gold compounds was assessed through ^{31}PNMR. Spectra were acquired both in DMSO-d_6 and in a mixture 9:1 of buffer phosphate (50 mM, pH 7.4) and DMSO-d_6 at 0, 24 h, 48 h and 72 h.

For both AFCN and AFSCN it is possible to observe a ligand displacement process leading to the formation of the $[Au(PEt_3)]^+$ cation.

Moreover, when solubilized in pure dimethyl sulfoxide, AFSCN allows the formation of a new species detected at 33.9 ppm in ^{31}P-NMR. This

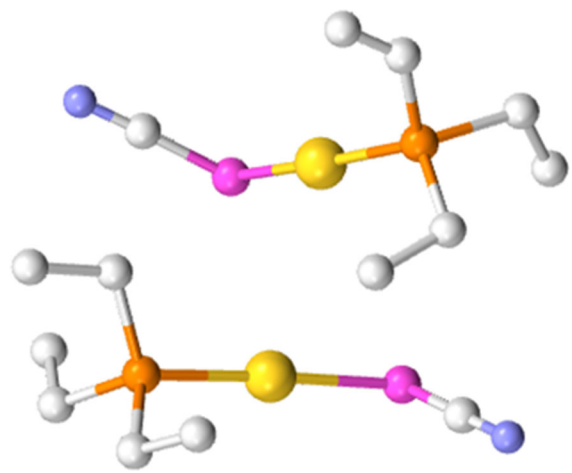

Fig. 2 The crystal structure of AFSCN

species was identified through ESI–MS investigation as a binuclear cation with raw formula of $[Au_2(PEt_3)_2SCN]^+$ (see supporting information, Fig. S14). Conversely, no spectral changes were observed in the same conditions for AFN_3 (see Figs. S15, S16).

Interactions with BSA monitored by ^{31}PNMR measurements

The interactions of $Au(PEt_3)CN$, $Au(PEt_3)SCN$ and $Au(PEt_3)N_3$ with BSA were previously analysed by ESI–MS in a methodological study (Pratesi et al. 2018). This study and its results have now been complemented by independent ^{31}PNMR measurements.

^{31}PNMR experiments were carried out on samples where 35 mg of BSA were mixed with one equivalent of $Au(PEt_3)X$ (X = CN; SCN; N_3) and solubilised under controlled temperature through sonication in 0.5 mL of D_2O. The spectra were acquired at t_0 and after 24 h of incubation at 37 °C, pH was checked at the end of each measurement and no changes were found. As reported in Fig. 5, AFCN (36.5 ppm) reacted immediately with BSA forming an $AlbSAuPEt_3$ derivative. The latter species is characterized by a ^{31}PNMR signal located at 42.0 ppm (Isab et al. 1988b; Coffer et al. 1987; Isab et al. 1988a); during this reaction a conspicuous amount of the $[Au(PEt_3)_2]^+$ cation (47.0 ppm) was formed that is usually found in tiny amounts as a side product (Marzo et al. 2017; Coffer et al. 1986). The formation of $[Au(PEt_3)_2]^+$ can be easily explained by the scrambling reaction of AFCN described in literature, accompanied by the formation of the $[Au(CN)_2]^-$ anion (Marzo et al. 2017). Noteworthy, the discrepancy (3 ppm) in the chemical shifts of the detected species in comparison with those reported in literature (Isab et al. 1988a, b; Coffer et al. 1987; Coffer et al. 1986) is the consequence of a calibration in the NMR experiments on $OP(OCH_3)_3$ instead on H_3PO_4. The equilibrium constant for the reaction that these systems undergo, was shown to be dependent upon the solvent, increasing with the polarity and/or polarizability of the solvent itself (Marzo et al. 2018).

After 24 h of incubation the presence of the $AlbSAuPEt_3$ adduct was still detected. Furthermore, a complete disappearing of both free AFCN and the Au-diphosphine cationic scrambling product was observed, as well as the concomitant formation of $POEt_3$ specie. These data let us to confirm the mechanism proposed for the binding of AFCN to albumin (Isab et al. 1988a).

On the whole, the Au/BSA interaction process can be summarised as below:

(1) AFCN releases the CN^- anion when the bound with thiolic residue in Cys34 takes place.
(2) The $AlbSAuPEt_3$ adduct releases a phosphine molecule triggered by the reaction with the cyanide anion generated in the first step, leading to the formation of a new AlbSAuCN adduct.
(3) The released phosphine moiety was finally oxidized to the corresponding triethylphosphine oxide, likely provoking the subsequent reduction of some disulphide bridges present in BSA (Fig. 3).

Despite the similarity of their chemical structures, the reactivity of AFSCN turned out to be different respect to AFCN. Indeed, upon incubating AFSCN in the same condition, a quantitative formation of $AlbSAuPEt_3$ adduct was observed at t_0 (Fig. 4). Moreover, after 24 h of incubation a more complex speciation was detected. Indeed, it was possible to observe the formation of a small amount of $[Au(PEt_3)_2]^+$ cation, a backformation of AFSCN (broad signal at 38.1 ppm) and the generation of the dinuclear cation $[Au_2(PEt_3)_2SCN]^+$ at 32.9 ppm.

AFN_3 was also analysed following the same experimental protocol. As reported in Fig. 5, and similarly to AFSCN, AFN_3 turned out to give a rapid and quantitative formation of $AlbSAuPEt_3$ adduct at t_0 and after 24 h of incubation no changes were detected in the spectrum. This lack of further reactivity during the incubation was probably due to the lower affinity of the released azido group towards Au(I) compared to the cyanide or thiocyanate anions. In fact, the released azido residue seemed to be unable to further interact with the formed $AlbSAuPEt_3$ adduct.

Cytotoxicity assays

The cytotoxic effects of the three compounds were assessed in vitro toward a representative CRC cell line, HCT116 (Fig. 6 and Supporting Material). The effects were tested by the trypan blue exclusion assay, after 24 h of incubation. First of all, single dose experiments were carried out on the ground of the IC_{50}

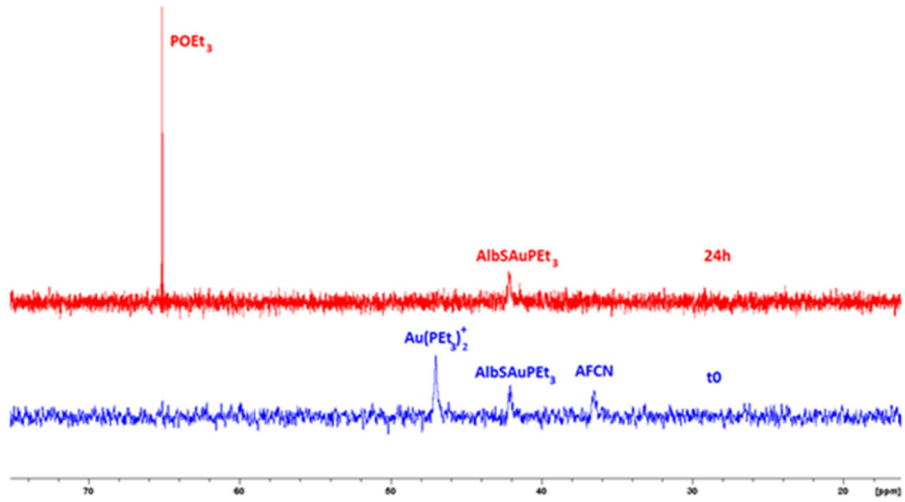

Fig. 3 NMR Spectrum of AFCN 1 mM + BSA 1 mM in D_2O at t_0 (blue) and after 24 h of incubation at 37 °C (red). (Color figure online)

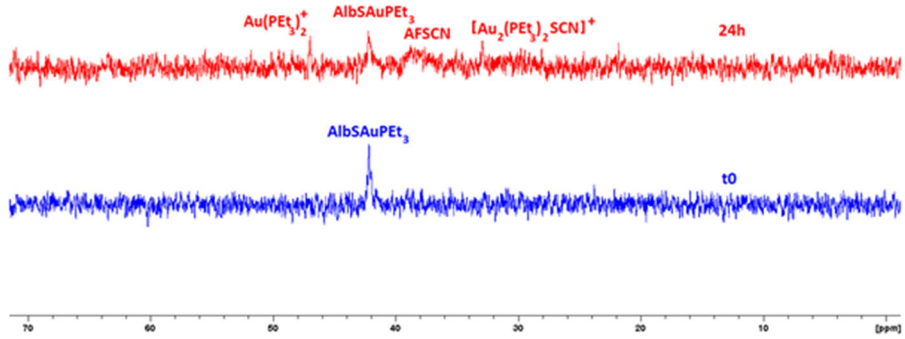

Fig. 4 NMR Spectrum of AFSCN 1 mM + BSA 1 mM in D_2O at t_0 (blue) and after 24 h of incubation at 37 °C (red). (Color figure online)

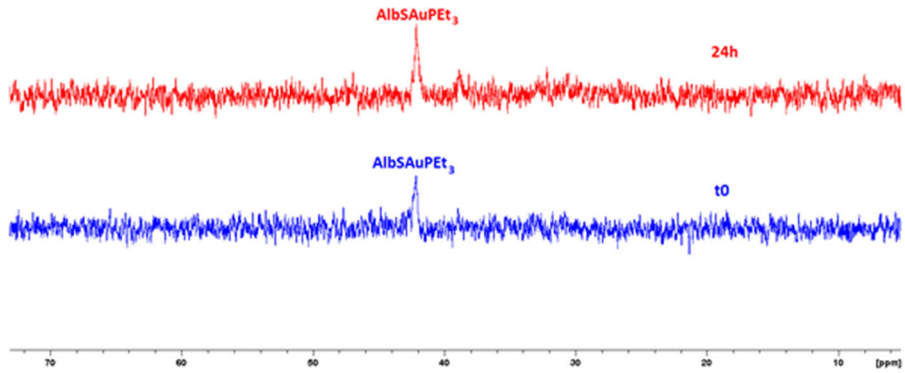

Fig. 5 NMR Spectrum of AFN_3 1 mM + BSA 1 mM in D_2O at t0 (blue) and after 24 h of incubation at 37 °C (red). (Color figure online)

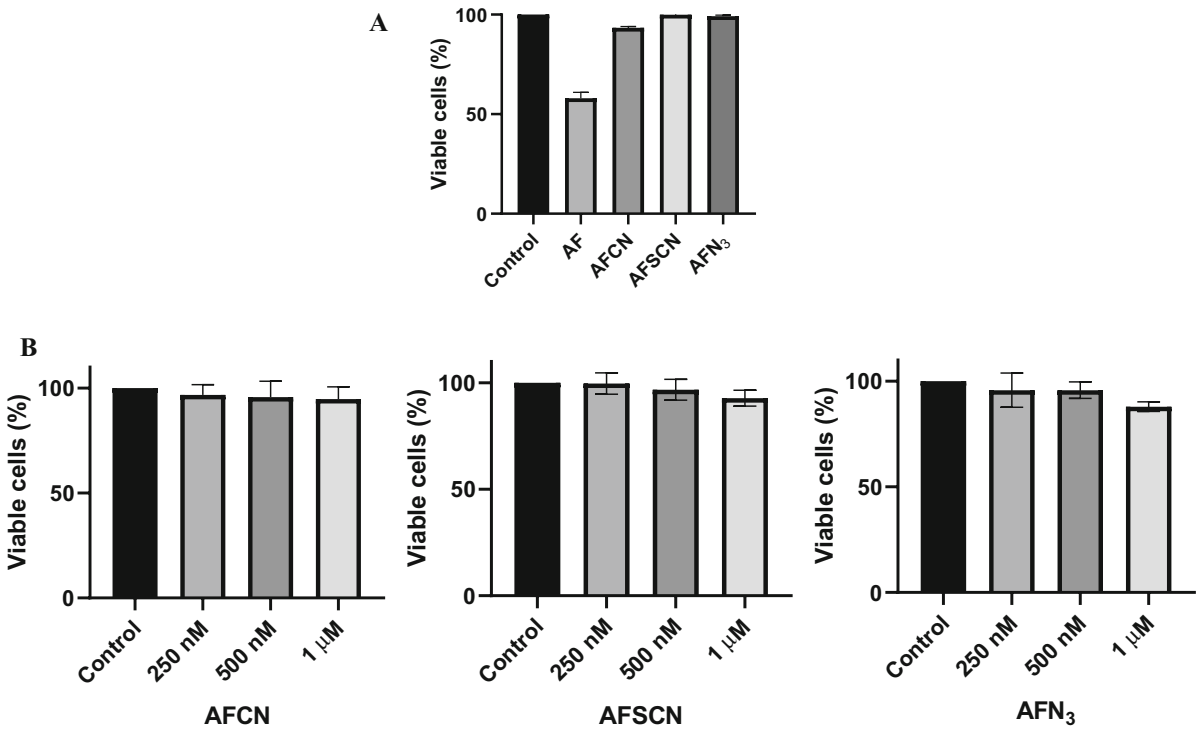

Fig. 6 Evaluation of cytotoxic activity of AFCN, AFSCN and AFN_3 in HCT116 cells. Cell viability was investigated after 24 h of treatment by the trypan blue exclusion assay. The column graphs represent the effect of the compounds in term of percentage of viable HCT116 cells. Viable cells were counted in triplicate, using a haemocytometer. **a** AFCN, AFSCN and AFN3 were tested at a representative concentration i.e. IC_{50} of AF, 180 nM. **b** The compounds, respectively AFCN, AFSCN and AFN_3, were tested at 250 nM, 500 nM and 1 μM

value of AF, which has been recently published by our group (Marzo et al. 2017).

We observed that the three compounds did not exert a remarkable activity at 180 nM (being this the value of AF IC_{50} HCT116 cells in the same experimental condition). Only AFCN shows a slightly cytotoxic action (Fig. 6a).

Thus, we decided to expose HCT116 cells to greater concentrations of the three study compounds: 250 nM, 500 nM up to 1 μM ($\sim$ 5 times higher than IC_{50} of AF). However, AFCN, AFSCN and AFN_3 do not show relevant cytotoxic proprieties even at these concentrations (Fig. 6b).

In a third experiment we exposed HCT116 cells to a 10 μM concentration of the three study compounds; in this latter case we observe nearly complete inhibition of cell growth. These results suggest that the IC_{50} values of the three compounds are almost comparable in the three cases and roughly fall in the concentration interval 3–8 μM. Thus, AFCN, AFSCN and AFN_3 appear to be far less active than AF but still remarkably cytotoxic with IC50 values < 10 μM.

Conclusions

Here, we have reported on the synthesis and the chemical characterization of three AF derivatives where the thiosugar ligand is replaced by a pseudo-halide ligand, i.e. cyanide, thiocyanate and azide, respectively. For one of them i.e. AFSCN, the crystal structure has been solved revealing a classical linear coordination at the gold(I) center in line with expectations. The solution behaviour of these gold compounds was analysed comparatively by ^{31}PNMR. This analytical technique permits to monitor the stability and the chemical transformations. Moreover, ^{31}PNMR was also exploited to analyse the molecular interactions of these gold compounds with bovine serum albumin. Lastly, these compounds were studied for their antiproliferative properties toward the HCT116

cancer cell line. Results revealed quite different pharmacological profiles: notably, the replacement of the thiosugar with a pseudohalide did not lead to loss of the biological activity confirming that the thiosugar moiety is not essential for pharmacological activity, in line with previous observations on the halide derivatives (Marzo et al. 2017). Rather, we observed some remarkable attenuation of the cytotoxic properties; these results clearly imply that the nature of the anionic ligand can modulate heavily the pharmacological activity of $Au(PEt_3)X$ metal complexes, suggesting that the biological profile could be improved with simple chemical modifications of the molecule. Indeed, the overall activity of the metal complex is significantly linked to the nature of X^- group, that is reasonable to assume to be acting as the leaving group. The affinity of the ligands toward the gold centre strongly affects the existing equilibria with an important impact into the pharmacological effects that are exerted by the active cationic species $[Au(PEt_3)]^+$. Additionally, differences in the antiproliferative actions may be broadly correlated with differences in the reactivity with target proteins. To this end the study of the interactions with BSA here reported may represent a simple and instructive model.

Acknowledgements D.C. gratefully acknowledge Associazione Italiana per la Ricerca sul Cancro for the financial support (AIRC 1-year Fellowship for Italy—Project Code: 22294). L.M. gratefully acknowledges AIRC (Associazione Italiana per la Ricerca sul Cancro) and ECRF (Ente Cassa di Risparmio di Firenze) for the financial support (AIRC-ECRF19650). CIRCMSB and ente CRF are also acknowledged. T.M. thanks University of Pisa (Rating Ateneo 2018/2019) for the financial support.

References

Allen FH (2002) The Cambridge structural database: a quarter of a million crystal structures and rising. Acta Crystallogr B58:380–388

Altomare A, Burla MC, Camalli M, Cascarano GL, Giacovazzo C, Guagliardi A, Moliterni AGG, Polidori G, Spagna R (1999) SIR97: a new tool for crystal structure determination and refinement. J Appl Crystallogr 32:115–119

Blocka KLN, Paulus HE, Furst DE (1986) Clinical pharmacokinetics of oral and injectable gold compounds. Clin Pharmacokinet 11:133–143

Cirri D, Pillozzi S, Gabbiani C, Tricomi J, Bartoli G, Stefanini M, Michelucci E, Arcangeli A, Messori L, Marzo T (2017) PtI_2(DACH), the iodido analogue of oxaliplatin as a candidate for colorectal cancer treatment: chemical and biological features. Dalton Trans 46:3311–3317

Coffer MT, Shaw CF III, Eidsness MK, Watkins JW II, Elder RC (1986) Reactions of auranofin and chloro(triethylphosphine)gold with bovine serum albumin. Inorg Chem 25:333–339

Coffer MT, Shaw CF III, Hormann AL, Mirabelli CK, Crooke ST (1987) Thiol competition for Et_3PAuS-albumin: a nonenzymatic mechanism for Et_3PO formation. J Inorg Biochem 30:177–187

CrysAlisPro 1.171.38.41r, (2015) Rigaku Oxford Diffraction

Database of privately and publicly funded clinical studies conducted around the world. https://clinicaltrials.gov

El-Etri MM, Scovell WM (1990) Synthesis and spectroscopic characterization of (triethylphosphine)gold(I) complexes $AuX(PEt_3)$ (X = Cl, Br, CN, SCN), $[AuL(PEt_3)^+]$ (L = SMe_2, $SC(NH_2)_2$, H_2O), and (μ-S)$[Au(PEt_3)]_2$. Inorg Chem 29:480–484

Fabbrini MG, Cirri D, Pratesi A, Ciofi L, Marzo T, Guerri A, Nistri S, Dell'Accio A, Gamberi T, Severi M, Bencini A, Messori L (2019) A fluorescent silver(I) carbene complex with anticancer properties: synthesis, characterization, and biological studies. Chem Med Chem 14:182–188

Fanali G, di Masi A, Trezza V, Marino M, Fasano M, Ascenzi P (2012) Human serum albumin: from bench to bedside. Mol Aspects Med 33:209–290

Farrugia LJ (1997) ORTEP-3 for Windows—a version of ORTEP-III with a Graphical User Interface (GUI). J Appl Crystallogr 30:565

Farrugia LJ (2012) WinGX and ORTEP for Windows: an update. J Appl Crystallogr 45:849–854

Hormann-Arendt AL, Shaw CF III (1990) Ligand-scrambling reactions of cyano(trialkyl/triarylphosphine)gold(I) complexes: examination of factors influencing the equilibrium constant. Inorg Chem 29:4683–4687

Hou GX, Liu PP, Zhang S, Yang M, Liao J, Yang J, Hu Y, Jiang WQ, Wen S, Huang P (2018) Elimination of stem-like cancer cell side-population by auranofin through modulation of ROS and glycolysis. Cell Death Dis 9:89–103

Isab AA, Hormann AL, Coffer MT, Shaw CF III (1988a) Reversibly and irreversibly formed products from the reactions of mercaptalbumin (AlbSH) with Et_3PAuCN and of $AlbSAuPEt_3$ with HCN. J Am Chem Soc 110:3278–3284

Isab AA, Shaw CF III, Hoeschele JD, Locke J (1988b) Reactions of trimethylphosphine analogs of auranofin with bovine serum albumin. Inorg Chem 27:3588–3592

Landini I, Lapucci A, Pratesi A, Massai L, Napoli C, Perrone G, Pinzani P, Messori L, Mini E, Nobili S (2017) Selection and characterization of a human ovarian cancer cell line resistant to auranofin. Oncotarget 8:96062–96078

Lee P, Wu X (2015) Review: modifications of human serum albumin and their binding effect. Curr Pharm Des 21:1862–1865

Marcon G, Messori L, Orioli P, Cinellu MA, Minghetti G (2003) Reactions of gold(III) complexes with serum albumin. Eur J Biochem 270:4655–4661

Marzo T, Cirri D, Gabbiani C, Gamberi T, Magherini F, Pratesi A, Guerri A, Biver T, Binacchi F, Stefanini M, Arcangeli A, Messori L (2017) Auranofin, Et_3PAuCl, and Et_3PAuI are highly cytotoxic on colorectal cancer cells: a chemical and biological study. ACS Med Chem Lett 8:997–1001

Marzo T, Cirri D, Pollini S, Prato M, Fallani S, Cassetta MI, Novelli A, Rossolini GM, Messori L (2018) Auranofin and its analogues show potent antimicrobial activity against multidrug-resistant pathogens: structure–activity relationships. ChemMedChem 13:2448–2454

Marzo T, Massai L, Pratesi A, Stefanini M, Cirri D, Magherini F, Becatti M, Landini I, Nobili S, Mini E, Crociani O, Arcangeli A, Pillozzi S, Gamberi T, Messori L (2019) Replacement of the thiosugar of auranofin with iodide enhances the anticancer potency in a mouse model of ovarian cancer. ACS Med Chem Lett 10:656–660

Massai L, Pratesi A, Gailer J, Marzo T, Messori L (2019) The cisplatin/serum albumin system: a reappraisal. Inorg Chim Acta 495:118983–118989

May HC, Yu JJ, Guentzel MN, Chambers JP, Cap AP, Arulanandam BP (2018) Repurposing Auranofin, Ebselen, and PX-12 as antimicrobial agents targeting the thioredoxin system. Front Microbiol 9:336–345

Nardelli M (1995) PARST95—an update to PARST: a system of Fortran routines for calculating molecular structure parameters from the results of crystal structure analyses. J Appl Crystallogr 28:659

Pratesi A, Cirri D, Ciofi L, Messori L (2018) Reactions of auranofin and its pseudohalide derivatives with serum albumin investigated through ESI-Q-TOF MS. Inorg Chem 57:10507–10510

Pushpakom S, Iorio F, Eyers PA, Escott KJ, Hopper S, Wells A, Doig A, Guilliams T, Latimer J, McNamee C, Norris A, Sanseau P, Cavalla D, Pirmohamed M (2019) Drug repurposing: progress, challenges and recommendations. Nat Rev Drug Discov 18:41–58

Roder C, Thomson MJ (2015) Auranofin: repurposing an old drug for a golden new age. Drugs R D 15:13–20

Singh N, Pagariya D, Jain S, Naik S, Kishore N (2018) Interaction of copper (II) complexes by bovine serum albumin: spectroscopic and calorimetric insights. J Biomol Struct Dyn 9:2449–2462

Sokołowska M, Wszelaka-Rylik M, Poznański J, Bal W (2009) Spectroscopic and thermodynamic determination of three distinct binding sites for Co(II) ions in human serum albumin. J Inorg Biochem 103:1005–1013

Talib J, Beck JL, Ralph SF (2006) A mass spectrometric investigation of the binding of gold antiarthritic agents and the metabolite $[Au(CN)_2]^-$ to human serum albumin. J Biol Inorg Chem 11:559–570

Thorn A, Dittrich B, Sheldrick GM (2012) Enhanced rigid-bond restraints. Acta Crystallogr A68:448–451